# 3-D seismic detection of undrilled prospective areas in a mature province, South Marsh Island, Gulf of Mexico

*MICHAEL V. DEANGELO and LESLI J. WOOD, Bureau of Economic Geology, Austin, Texas, U.S.*

This paper focuses on the most effective approach to defining additional resources using 3-D seismic as the sole data source. Although this example is from a densely drilled province, such a seismic-based approach is often used in frontier areas with sparse well coverage, in step-out regions around known production, can be used for a "quick look" evaluation of existing properties, and for real-time interpretation of newly acquired data.

This approach—integrating multiple seismic attributes and interpretation methods—refined the structural framework and detected undrilled prospective areas in a mature province in the Gulf of Mexico. Coherency technologies refined the fault interpretations. Surface mapping identified structural highs, and stratal-surface techniques were used to evaluate seismic stratigraphic facies.

The study area covered approximately 350 square miles of coastal waters just south of Marsh Island, Louisiana (Figure 1). Data consisted of two merged 3-D surveys, Outer Continental Shelf (OCS) 310 and State Lands (SL) 340 that cover six productive offshore fields: Starfak, Tiger Shoal, Mound Point, Amber Complex, Lighthouse Point, and North Lighthouse Point.

The area is in the Oligocene-Miocene detachment province of the northern Gulf Coast continental margin—a region generally characterized by large-displacement, dominantly down-to-the-basin, listric growth faults that sole on a regional detachment zone above the Oligocene section. Regional deformation is a product of salt mobilization. The faults originate in the autochthonous Jurassic Louann Salt or in the detachment zone represented by a salt weld that formerly contained a thick, allochthonous salt body.

A characteristic feature of this province is the thickness (typically exceeding three miles) of deltaic and shelf sediments above the detachment zone. This remarkable stacking of deltaic/shelf sandstone reservoirs helps make this province one of the world's great petroleum provinces (Table 1). More than 500 wells within the seismic coverage document proven and remaining hydrocarbon reserves (Figure 2, composite log of Tiger Shoal/Starfak fields).

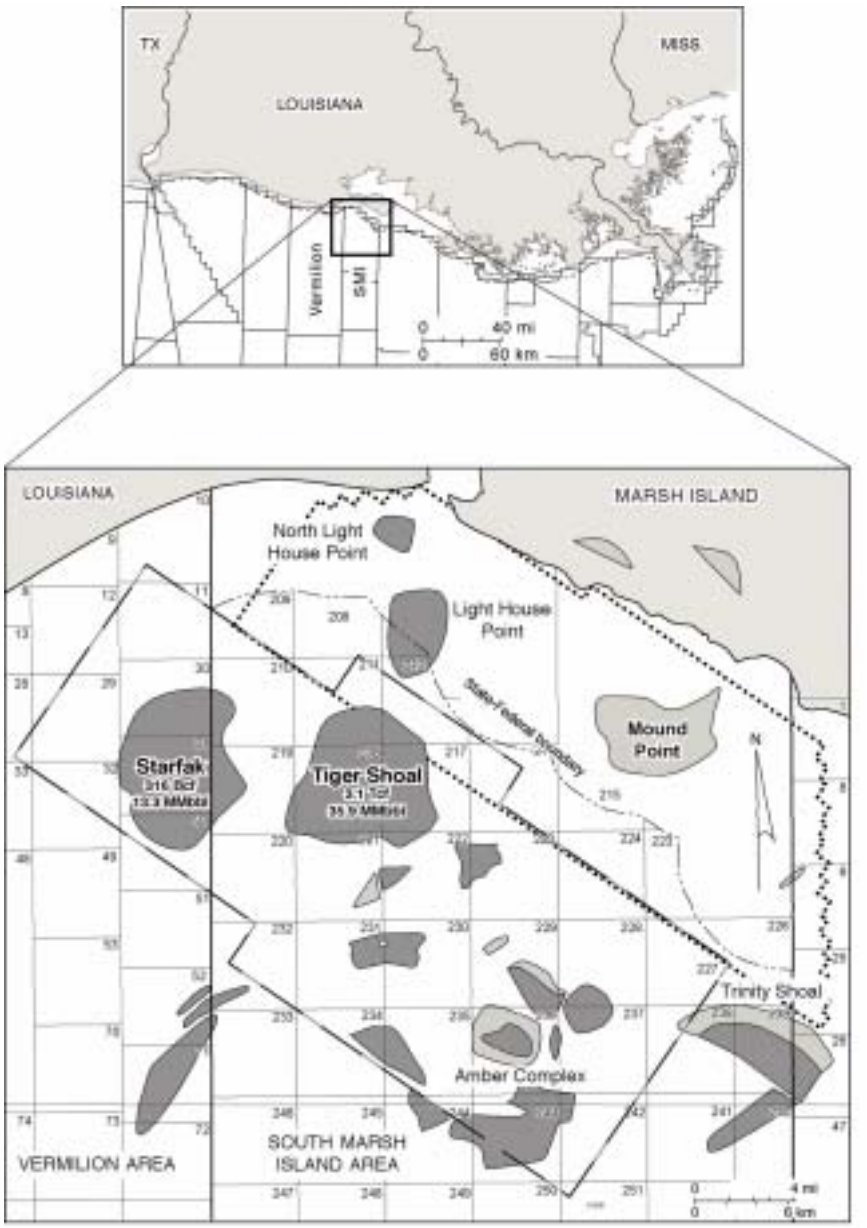


**Figure 1. Tiger Shoal area in Vermilion Block 50 offshore Louisiana. Surrounding fields and the outline of the two major 3-D seismic surveys are indicated.**

**Fault interpretation methods.** Coherence time slices were used in the initial structural interpretation phase because this technology allows a mathematical assessment of the 3-D seismic data volume without being biased by previous interpretation. Coherence calculations compare

waveform similarity between adjacent traces. Traces within a specified time window are crosscorrelated with neighboring traces. The lowest correlation coefficient calculated will be assigned to the central sample.

Coherence values range from +1 to -1. A value of +1 indicates a perfect match between adjacent traces. Coherence values near +1 indicate no lateral variations in stratigraphy or structure. A value of -1 indicates significant trace similarity if the phase of one of the waveforms is inverted. This condition could be an indicator of offset (faulting) within the reference window. A coherence value of zero indicates no correlation between seismic reflection character. Low coherence values (either positive or negative) may indicate significant lateral changes in rock type, pore fluid content, faulting, or any geologic parameter that can affect seismic reflection waveshapes.

Fault segments are more pronounced on coherence time slices (Figure 3) relative to conventional amplitude time slices (Figure 4). Time slices of the coherency volume, starting at 2000 ms, were generated at 100-ms intervals. Fault segments were identified and mapped across each of these slices. Vertical seismic sections oriented in dip direction were then extracted from the 3-D seismic amplitude volume for analysis. The fault segments identified from the coherence time slices were projected onto these extracted dip seismic sections so fault segments could be correlated to a particular fault line in the vertical seismic section.

Analysis of the 3-D seismic volume reveals numerous normal faults throughout the area. At least five first-order normal faults extend from near the seafloor to below seismic depth coverage (Figure 5). First-order growth faults are characterized by increasingly thicker hanging-wall sequences of sediments as depth increases. These five faults have several deep rollover features that are potential drilling targets. In addition, second-order faults were interpreted from the coherency slices.

**Table 1. Distribution of reserves and production data by geologic age for the Gulf of Mexico, showing the Miocene-age reservoir resources leading all categories, including remaining proved reserves**

| Age | Original proved reserves (percent) | Cumulative production (percent) | Remaining proved reserves (percent) |
|---|---|---|---|
| Pleistocene | 40 | 41 | 37 |
| Pliocene | 16 | 16 | 16 |
| Miocene | 42 | 43 | 41 |
| Oligocene, Cretaceous, and Jurassic | 2 | 0 | 6 |

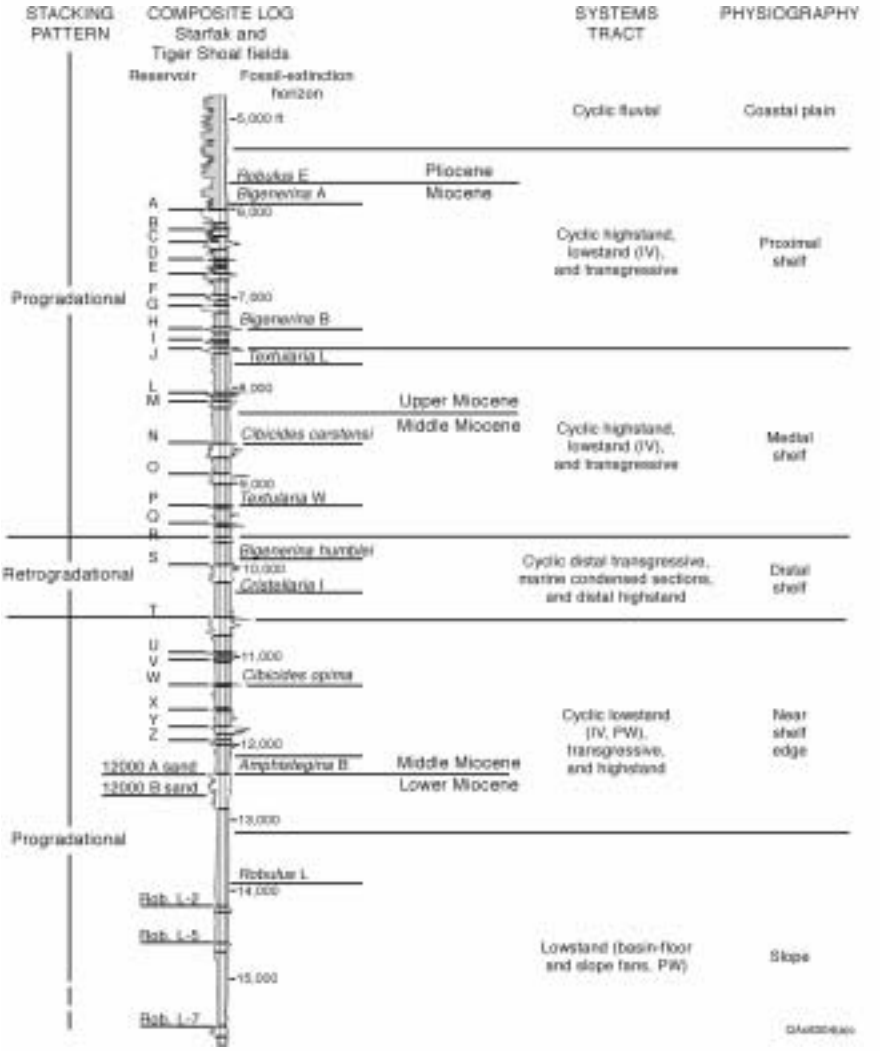


**Figure 2. Composite type log of Starfak and Tiger Shoal fields that displays gross stacking patterns, reservoir nomenclature, extinction horizons of invertebrate paleofauna, and stage boundaries.**

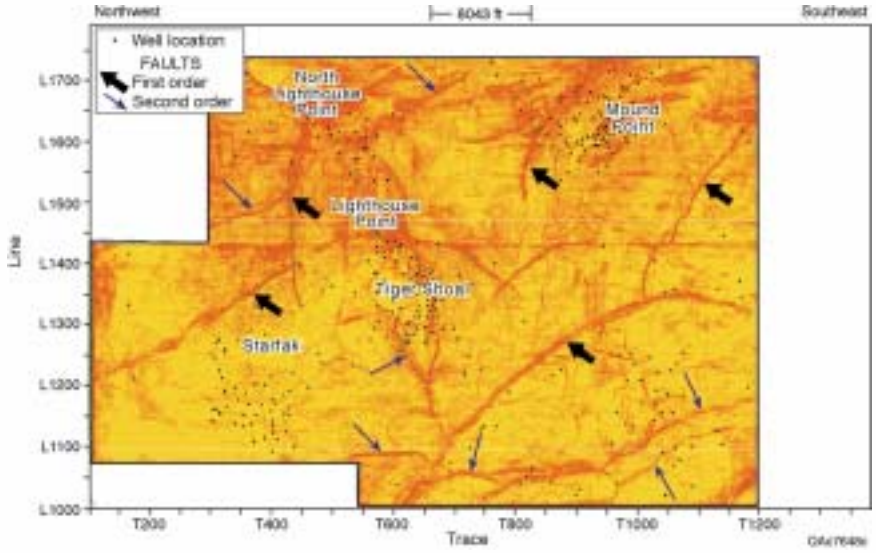


**Figure 3. Coherency time slice at 2000 ms reveals spatial distribution of faulting throughout the 3-D seismic study area.**

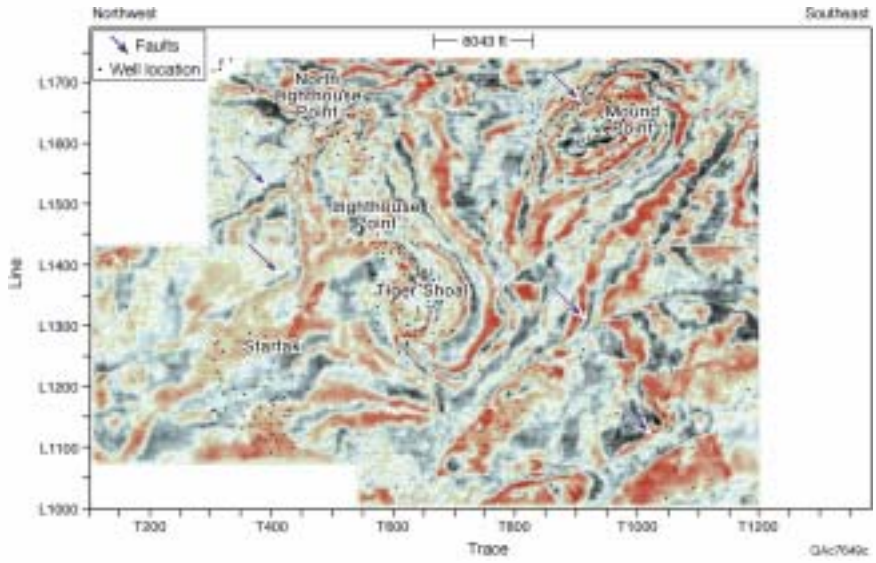


**Figure 4. Conventional time slice (2000 ms) from the 3-D seismic amplitude volume.**

Second-order faults generally have less offset (<200 ft) than first-order faults; however, significant hydrocarbons may still trap within these three-way closures.

**Surface mapping methods.** Maximum flooding surfaces (i.e., condensed sections) provide time-marker surfaces for mapping chronostratigraphic packages throughout the study area. These surfaces are characterized by both continuity and high amplitude. They are often downlapped by overlying reflectors, typical of condensed sections in the Gulf Coast. Examination of well data supports the interpretation of these surfaces as major regional flooding events that are likely to be pervasive throughout the northern Gulf. This increases the likelihood that these surfaces will be useful outside of the immediate area.

These surfaces are easily mapped with high confidence within fault blocks. Difficulties still arise in correlation of surfaces across first-order growth faults that occur in close association with the paleoshelf edge.

Shelf edges are recognizable by dramatic stratigraphic expansion to the south-southeast across short distances. Because of the ambiguity of correlating footwall flooding events (updip) with hanging-wall flooding events (downdip), it was decided to begin mapping in areas of minimum fault throw to provide a higher level of cross-fault correlation confidence. Arbitrary loop displays were extensively employed to ensure maximum confidence in surface correlation. Subsequent mapping continued into northern parts of the area and stopped at the major growth fault associated with the shelf edge. The mapping surface was then correlated over the large growth fault in the northeast by comparing vertical seismic polygon displays extracted from footwall events with corresponding hanging-wall events. This allowed the interpreter to take advantage of the minimal amount of structural offset present. The mapping surface was then extended to the south and terminated in the south-central sector of the area. All surfaces mapped in the 3-D seismic data followed this approach.

**Structural mapping and fault interpretation.** Time structure maps show several structural high points. Tiger Shoal and Mound Point fields are structurally high and dominated by crestal fault-bounded grabens. Lighthouse Point and North Lighthouse Point are in the central, northwestern portions of the area. Starfak Field is a subregional high point in the south-southwestern portion. These structural highs have been heavily targeted for hydrocarbon exploitation. Within each field, normal faults play a significant role in hydrocarbon partitioning. All topographical features are conformable to depth and impact structural plays into the early Miocene.

The area is dominated by normal, extensional faulting, with no evidence of compression. A significant first-order growth fault (A in Figure 6) crosses E-W through the middle of the area and forms the northern boundary of Starfak and Tiger Shoal. North of Starfak, this fault has offsets greater than 350 ft. Producing reservoir sands are on the downthrown side of this fault. Offsets decrease (<250 ft) in Tiger Shoal and contain reservoir-quality sands on both sides of the fault.

A north-south trending first-order fault (B) separates Lighthouse Point and North Lighthouse Point. This fault forms the western boundary of Lighthouse Point and has offsets greater than 350 ft. Mound Point is bounded on the western edge by a first-order normal fault (C). The fault trends away from the southwestern portion of Mound Point and extends to the northeast beyond 3-D seismic coverage.

The majority of reservoir-quality sands is interpreted to be on the downthrown side of this fault. Two first-order growth faults (D and E) separate

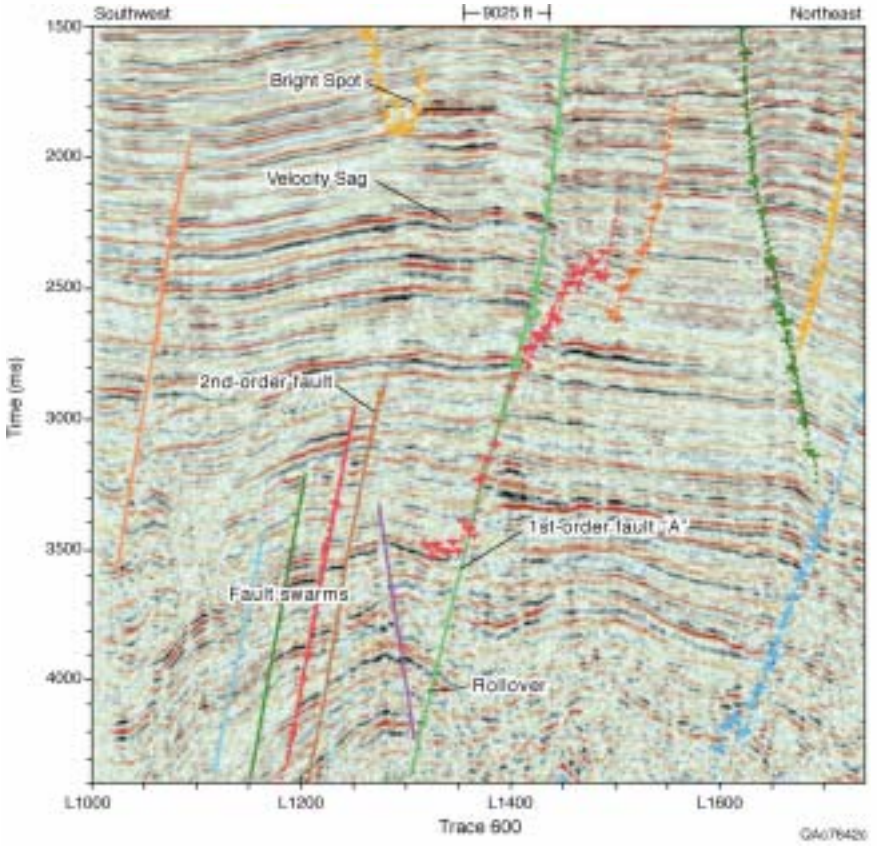


**Figure 5. Vertical seismic section (squash plot, i.e. horizontally compressed) showing structural (rollover), stratigraphic (bright spot), and fault interpretations of first- and second-order normal faults.**

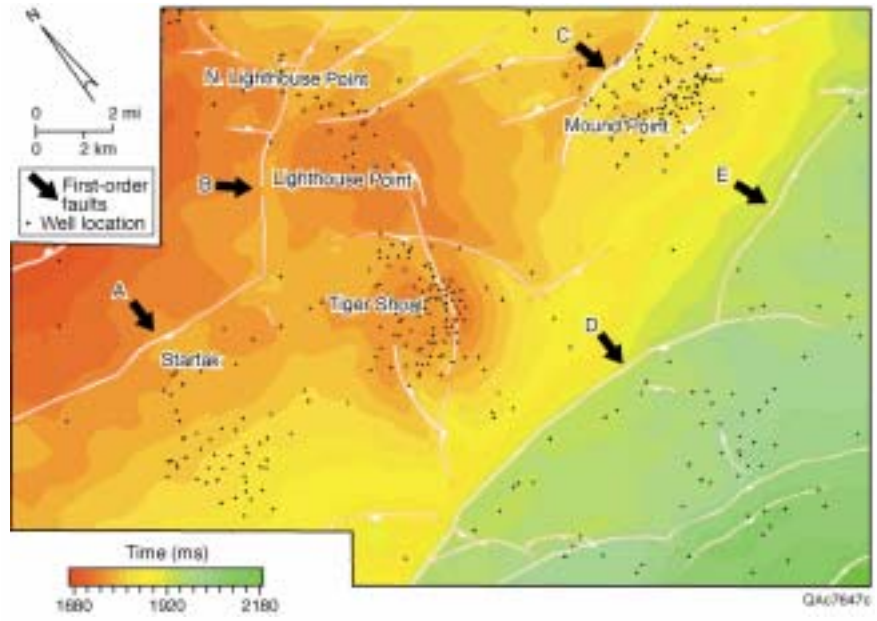


**Figure 6. Time structure map (contour interval = 20 ms) of maximum flooding surface 2 depicting the subsurface topography associated with the five major producing fields. Note the five (A, B, C, D, and E) first-order normal faults.**

important fault bounded basins in the southern and southeastern portions of the area from the five major fields in the western and northern portions. These two faults, characterized by offsets (>500 ft) that increase with depth and thickening basinward deposits, are believed to correspond to the paleoshelf edge. Downdip deposits may offer good trend plays of stratigraphically trapped hydrocarbon accumulations that parallel the fault's strike. Additional fault complexes are evident throughout the study area and each has potential hydrocarbon accumulations.

First-order growth faults have many associated rollover features (Figure 5). Rollovers develop when beds in the hanging wall of the downthrown block are folded over by strata expansion along the growth fault. Rollovers are excellent targets for hydrocarbon accumulations. These features are commonly found in the deeper portions of first-order growth faults, where fault offset is greatest. The 3-D seismic volume was examined to pinpoint strong amplitude anomalies (bright spots) terminating against faults that may indicate hydrocarbon accumulations (Figure 7).

**Analysis of deep structural trends and facies.** Structure below 3200 ms (Figure 8) is more complex, and seismic data quality degrades rapidly below this level. Overpressured areas, characterized by an abrupt change in *P*-wave velocity and bulk density, are believed to strongly influence the quality of the deep seismic data. Within the zone of overpressure, seismic amplitudes do not correlate well with known hydrocarbon-bearing reservoirs. Consequently, amplitude data below this level were considered to be unreliable predictors of hydrocarbon trends.

Deep segments of first-order growth faults have significant offset (>600 ft) and syndepositionally influenced the distribution of reservoir quality sediments in the south-southeastern portion of the study area. Interpretation of seismic facies and key surfaces reveals the several prograding wedges deposited along the southern margin during sea-level lowstand (Figure 9). Lowstand wedges thicken to the south and form oval-shaped thicks that strike east-west. They are bounded at their base by a basal unconformity that truncates underlying reflectors on which mounded and chaotic and sigmoid seismic reflectors downlap. A strong, high-amplitude, continuous reflector that shows downlap of underlying reflectors overlies the progradational wedges. Several fault swarms of closely spaced, limited-offset, second-order normal faults cut these lowstand wedge deposits in the southern part of Starfak Field. These faults likely have significant influence on hydrocarbon migration and distribution within these features. In some cases, where offset is greater than sand thickness, these faults may

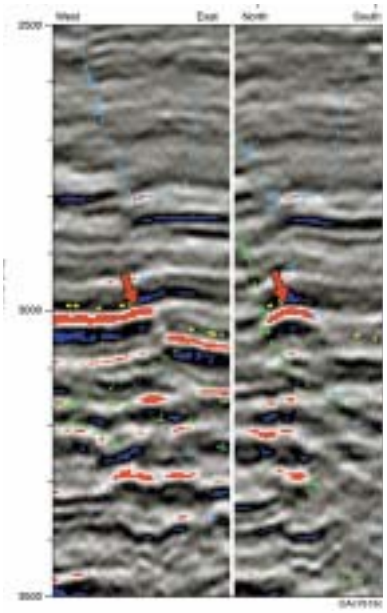

**Figure 7. Vertical seismic section (squash plot: horizontally compressed) of an undrilled structural lead, characterized by a strong amplitude anomaly (arrows) terminating against normal fault.**

form seals that impede the flow of hydrocarbons and form effective traps. In other cases, they may allow hydrocarbons to escape lowstand wedge systems and move along the faulted rock matrix to shallower reservoir intervals. Ongoing fault analysis in this area will reveal their individual roles.

**Stratal surface methods.** Stratal surface interpretation techniques were used to determine the spatial distribution of sandstone reservoirs. Stratal surfaces are visibly distinctive, chronostratigraphic, sheetlike rock units whose seismic signature parallels the acoustic impedance boundary associated with surrounding rock. Maximum flooding surfaces (MFS), pervasive throughout the area, served as excellent "stratal surfaces." These were subsequently used to define upper and lower extents of stratal-bounded seismic analysis windows (Figure 10). Facies-sensitive seismic attributes were extracted from between the mapped maximum flooding surfaces to generate paleolithologic maps (Figures 11 and 12), showing spatial lithologic relationships within a specified vertical (geologic time) zone of interest.

**RMS amplitudes and prospective areas.** Seismic reflection amplitude information can help identify unconformities, reefs, channel and deltaic sands, lithology, and gas/fluid accumulations. Amplitude anomalies may also be attributed to constructive or destructive interference (tuning effect) caused by two or more closely spaced reflectors and/or to variations in net sand within a thin-bed unit. RMS amplitudes are calculated as the square root of the average of the squares of the amplitudes found within an analysis window. The rms amplitudes are sensitive to sandstone-bearing depositional systems tracts within the reservoir-bearing successions and help define the spatial distribution of genetically related depositional successions. Such rms amplitude maps may image stratigraphic leads that have been missed by previous exploitation programs.

Calculating rms amplitudes between two bounding maximum flooding surfaces generated a map illuminating several depositional elements (Figure 11) associated with a

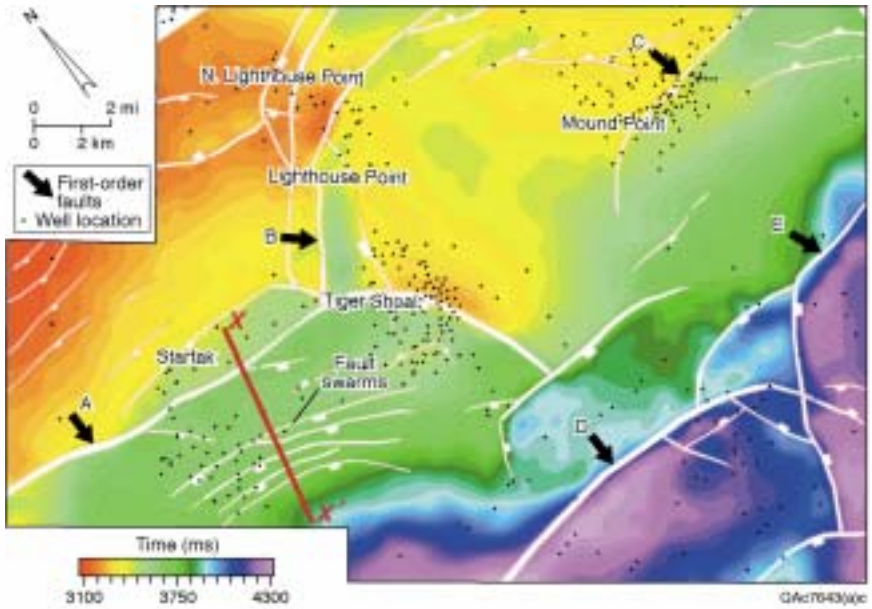


**Figure 8. Time structure map (contour interval = 25 ms) of the Robulus 4 sand with associated second-order fault swarms in Starfak Field.**

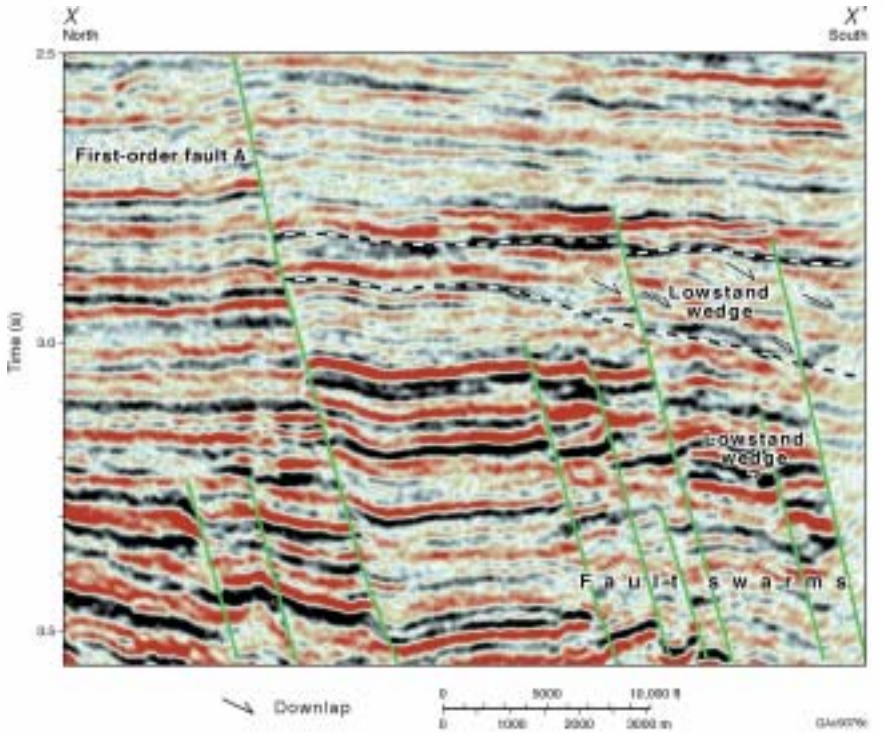


**Figure 9. Squash plot (horizontally compressed) cross-section showing seismic expression of lowstand system wedges.**

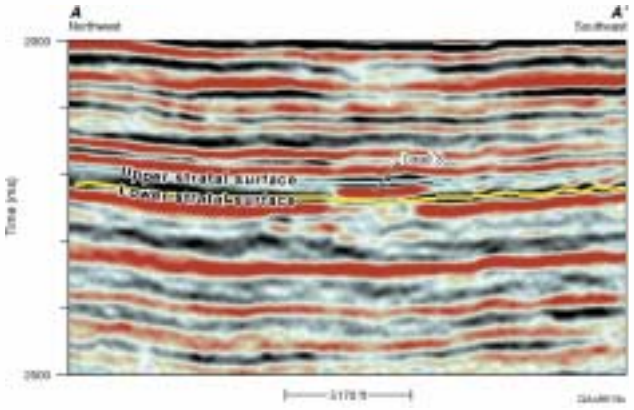


**Figure 10. Seismic cross-section showing stratal-surface analysis window used for generating rms amplitude map (Figure 12).**

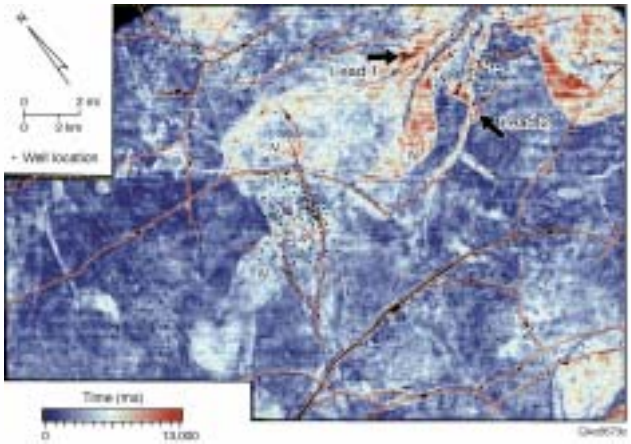


**Figure 11. An rms amplitude map of lowstand systems tract reservoir sands. Incised valley systems (IV) dominate the central portion of the study area.**

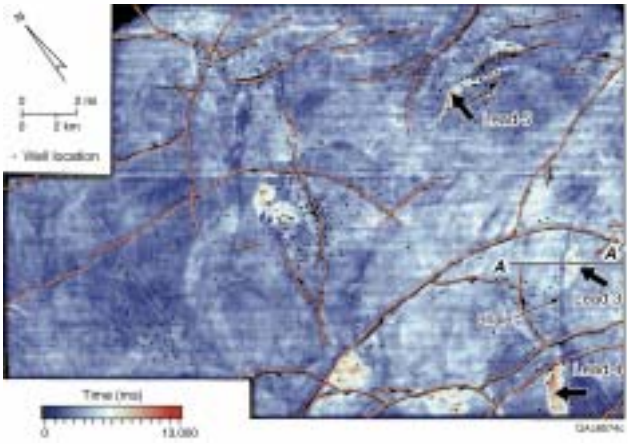


**Figure 12. An rms amplitude map of lowstand systems tract reservoir sands.**

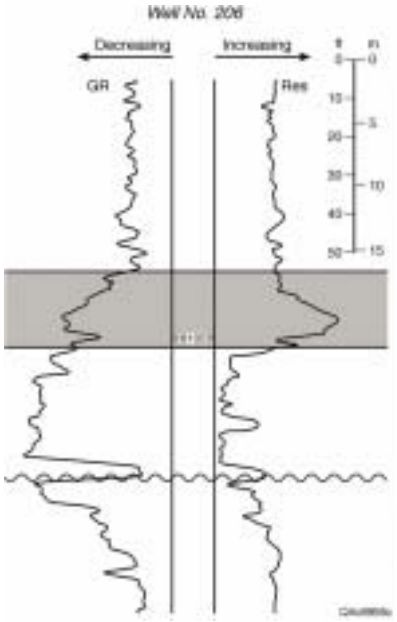


**Figure 13. Wireline log (gamma-ray and resistivity) from well 206. Upper 21 feet of reservoir (shaded area) is gas filled.**

lowstand systems tract reservoir. On this map, a large incised-valley system can be seen traversing the middle portion of the study area. Available well data indicated that this feature has been heavily exploited. Mound Point, however, has two promising leads previously overlooked by exploitation programs. The northernmost lead (lead 1) has a strong amplitude anomaly located on the downthrown block of a second-order growth fault (Figure 11). Associated faults have more than 100 ft of throw, which is likely sufficient to seal any hydrocarbon accumulations. The second lead (lead 2) is a sinuous feature interpreted to be remnants of an ancient fluvial system. Its strong amplitudes are on the upthrown block and truncate abruptly against a second-order

growth fault.

A second lowstand systems tract rms amplitude map (Figure 12) identified three possible additional leads. A strong amplitude anomaly (lead 3) on the downthrown block of a first-order growth fault is an excellent target. The sand body is interpreted to "shale out" or terminate before it reaches the first-order growth fault. A prominent dark blue lineation flanks the western edge of this anomaly and is interpreted to be a shale plug. To the immediate south of lead 3, an additional lead (lead 4) was identified. It is characterized by a strong amplitude anomaly bounded to the north by a second-order growth fault. Lead 5, in Mound Point Field, is characterized by a strong amplitude anomaly on a sinuous graben feature flanked on the north and south by second-order growth faults.

More than 20 stratigraphic leads were identified using rms amplitude maps generated for 18 separate reservoir levels. Often, vertical seismic sections fail to clearly identify these important stratigraphic features because they are typically manifested as subtle variations in amplitude strength, phase shift, or polarity reversal and are easily overlooked by interpreters. Imaging these leads in a horizontal view adds additional information of spatial distribution to the typical seismic cross-section geometries used to interpret seismic facies and thus infer depositional pattern that lend insight into the associated reservoir quality. The sinuous nature of these features can only be seen in such a horizontal view and well data from the area, as well as analogs from other fields, indicate that such sinuous features are highly likely to be incised valleys or channel reservoir sands.

**Well test results.** Texaco chose lead 3 as a drill site in its 2000 development program and spudded well OCS-G-0310 206 in 17 ft of water to test the stratigraphic trap identified on the corresponding rms amplitude map (Figure 12). The well was optimally located within the high-amplitude portion of this incised, low-sinuosity feature. Well results at the amplitude depth indicate a sharp-based fining upward gamma-ray signature interpreted to represent a 50-ft package of basal fluvial fill overlain by estuarine fill in the upper portions (Figure 13). This fill was overlain sharply by high gamma-ray, sealing shales of the overlying marine flooding event. The upper 21 ft of the reservoir interval was gas-filled, producing 3.5 million $ft^3/d$ with no condensate. Volumetrics subsequent to drilling indicate that the reservoir extent truly is limited to the north, suggesting that rms amplitude maps are accurate indicators of reservoir extent.

**Conclusions.** Applying methods that accurately define structure, stratigraphy, and regional trends in hydrocarbon accumulations allow leads and prospects for reserve growth opportunities to be developed expeditiously. Combining coherency technologies and stratal-surface mapping strategies enhances subsurface understanding. The accuracy of fault plane and fault polygon interpretation is improved by coherency technologies. If a better understanding of observations is required, commercial subsurface modeling software can import tightly constrained structural components with a minimum of editing. Stratal-surface methods often illuminate spatial distribution of important reservoir facies that are not easily recognizable in vertical seismic sections. Strategic infill-drilling programs in mature fields can be designed by analyzing maps generated by stratal-surface methods, specifically targeting undrilled prospective areas.

**Suggested reading.** "3-D seismic discontinuity for faults and stratigraphic features: The coherence cube" by Bahorich and Farmer (*TLE*, 1995). "3-D seismic stratal-surface concepts applied to the interpretation of a fluvial channel system deposited in a high-accommodation environment" by Hardage and Remington (GEOPHYSICS, 1999). "Assessment of conventional recoverable hydrocarbon resources of the Gulf of Mexico and Atlantic outer continental shelf: as of January 1, 1995" by Lore et al. (U.S. Department of the Interior, Minerals Management Service, Gulf of Mexico OCS Region, Office of Resource Evaluation, OCS Report MMS 99-0034, 1999). LE

*Acknowledgments: This article was prepared with the support of the U.S. Department of Energy under Cooperative Agreement DE-FC26-98FT40136. However, any opinions, findings, conclusions, or recommendations expressed herein are those of the author and do not necessarily reflect the views of the DOE. As an industry partner, Texaco contributed the well and 3-D seismic data. Landmark Graphics Corp. provided software for the basic 3-D seismic interpretation via the Landmark University Grant Program. Published with permission of the director, Bureau of Economic Geology, the University of Texas at Austin.*

*Corresponding author: michael.deangelo@beg.utexas.edu*